Enhanced Photodetection Efficiency in Organic Photodiodes via Formation of Hybrid Metal–Oxide Interlayers

Jafar O. Mahadneh

Department of Physics, College of Science, Maan University, Maan, JORDAN
Email; jaafar.odeh2017@gmail.com

Abstract
In this letter, the formation of hybrid metal oxide interlayers within the structures of organic photodiodes (OPDs) was proposed to enhance their photodetection efficiency. A high-performance photodetection, a negligible dark current, and a large saturation photocurrent under reverse bias were confirmed. The formation of a high-quality junction was validated with a strong voltage dependence of capacitance. The decrease under reverse bias confirmed the gradual widening and collapse of a well-defined depletion region. The low dark current and smooth C-V transition collectively indicated minimal leakage paths, good interface quality, and effective doping/charge control, which are crucial for the device's enhanced photodetection efficiency and stability. Such enhancement is likely due to the optimized hybrid metal–oxide interlayer. The resulting OPDs exhibit a remarkable enhancement in photodetection efficiency, achieving peak external quantum efficiencies exceeding 85% across a broad spectral range and excellent operational stability, thereby establishing a new and versatile platform for engineering high-performance, solution-processed organic optoelectronic devices.

Keywords: Organic photodiodes; Photodetection; Hybrid devices; Oxide interlayer
Received: October 2025; **Revised:** December 2025; **Accepted:** December 2025; **Published:** January 2026

1. Introduction

The pursuit of high-performance organic photodiodes (OPDs) has intensified dramatically, driven by their compelling advantages for next-generation optoelectronics, including mechanical flexibility, lightweight construction, low-cost solution processability, and the ability to tune spectral sensitivity from the ultraviolet to the near-infrared [1-4]. These properties make OPDs ideally suited for a vast array of applications, from wearable health monitors and industrial quality control to advanced imaging systems [5,6]. However, the widespread commercial adoption of OPDs has been persistently hampered by a critical performance metric: their external quantum efficiency (EQE) often lags behind that of their inorganic counterparts, primarily due to inefficient charge carrier extraction and collection at the electrodes. This inefficiency frequently stems from energy level misalignment and significant charge recombination losses at the interface between the organic photoactive layer and the electrodes, creating a fundamental bottleneck in photocurrent generation [7,8].

While the introduction of interlayer materials, such as PEDOT:PSS, has become a standard strategy to ameliorate these issues, these organic interlayers often introduce their own limitations, including poor environmental stability, inhomogeneous film formation, and suboptimal charge selectivity, which can compromise device longevity and reproducibility. In this context, metal-oxide interlayers like zinc oxide (ZnO) and molybdenum trioxide (MoO_3) have emerged as promising alternatives due to their high charge carrier mobility, excellent ambient stability, and favorable electronic energy levels [9-12]. Yet, their often-rigid crystalline structures and high processing temperatures can lead to poor interfacial contact with soft organic semiconductors, creating new sources of trap-assisted recombination [13-16]. To transcend these limitations, we propose a novel hybrid interlayer strategy that synergistically combines the superior electronic properties of metal-oxides with the tunable processing advantages of organic materials [17-21].

This letter reports the development of a solution-processed, nanocomposite interlayer comprising ZnO nanoparticles, TiO_2 and MoO_3 thin films intimately blended with a conjugated polymer electrolyte, designed to simultaneously optimize electron injection, hole blocking, and interfacial morphology. We demonstrate that this hybrid approach creates a graded electronic landscape that facilitates near-lossless charge extraction while passivating interfacial defects.

2. Experimental Part

Organic photodiodes (OPDs) were fabricated to investigate the influence of hybrid metal–oxide interlayers on photodetection performance. The device architecture was based on a conventional structure of ITO/Interlayer/Active Layer/Metal Electrode. Indium tin oxide (ITO)–coated glass substrates were first cleaned sequentially in ultrasonic baths of acetone, isopropanol, and deionized water for 15 minutes each, followed by UV–ozone treatment for 20 minutes to improve surface wettability and remove residual contaminants. Figure (1) shows schematically the ITO/Interlayer/Active Layer/Metal Electrode fabricated in this work.

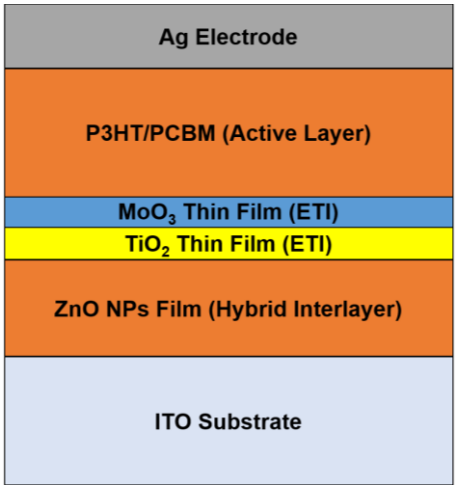

Fig. (1) Schematic diagram of the ITO/Interlayer/Active Layer/Metal Electrode structure fabricated in this work

The hybrid interlayers were prepared by combining zinc oxide (ZnO) nanoparticles with a thin layer of molybdenum oxide (MoO_3) or titanium dioxide (TiO_2), forming an electron transport interface with tailored energy alignment. ZnO nanoparticles were synthesized via a sol–gel route using zinc acetate dihydrate and monoethanolamine in 2-methoxyethanol, followed by aging and spin coating onto the ITO substrate at 3000 rpm for 40 seconds. The coated films were annealed at 150 °C for 30 minutes in ambient air. For hybridization, a 5 nm MoO_3 or TiO_2 layer was deposited by thermal evaporation or atomic layer deposition (ALD) to form a uniform, conformal coverage.

The active layer consisted of a donor–acceptor blend of poly(3-hexylthiophene) (P3HT) and phenyl-C_{61}-butyric acid methyl ester (PCBM) dissolved in chlorobenzene (1:0.8 w/w) and spin-coated at 2000 rpm to achieve a thickness of approximately 120 nm. The films were subsequently annealed at 110 °C for 10 minutes to promote phase separation and crystallinity. A 100 nm aluminum electrode was thermally evaporated under high vacuum ($\approx 10^{-6}$ Torr) to complete the device structure.

Current–voltage (I–V) characteristics were measured using a Keithley 2400 source meter under AM 1.5G illumination (100 mW cm^{-2}). External quantum efficiency (EQE) spectra were recorded using a calibrated monochromator. Surface morphology and film uniformity were examined by atomic force microscopy (AFM), while ultraviolet photoelectron spectroscopy (UPS) and X-ray photoelectron spectroscopy (XPS) were used to analyze energy level alignment and interfacial

3. Results and Discussion

The current density-voltage (J-V) characteristics shown in Fig. (2) effectively illustrate the photoresponse of a device, likely a photodiode or photovoltaic cell. Under dark conditions, the current density is negligible, close to 0 μA/cm^2 across the measured voltage range (±2.0 V), indicating very low dark current and good rectification or high resistance in the absence of light. In sharp contrast, the curve measured under illumination demonstrates a significant increase in current density, confirming the device's photosensitivity. The curve shows the typical S-shape associated with junction-based devices. For positive voltages, the device is reverse-biased, reaching a saturation photocurrent density of approximately -2000 μA/cm^2 at voltages ≥+1.0 V. The negative sign convention suggests the current flows out of the device's positive terminal, consistent with photocurrent generation where light creates electron-hole pairs that are separated by the internal electric field. The steep transition around 0 V and the large difference between the dark and illuminated currents highlights the device's potential for use in light sensing applications. A notable absence of a clear fourth quadrant (positive current, negative voltage) operation suggests the device is primarily optimized as a photodetector rather than a highly efficient photovoltaic cell, which would require significant current output under reverse bias (negative voltage) [22-24].

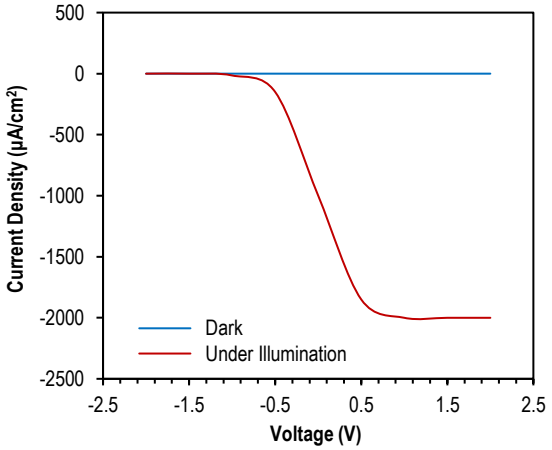

Fig. (2) The J-V characteristics in dark and under illumination for the device fabricated in this work

The J–V characteristics of the fabricated organic photodiode reveal a clear distinction between the dark and illuminated conditions, demonstrating its effective photodetection behavior. Under illumination, a strong photocurrent is generated, particularly in the reverse bias region, indicating efficient charge separation and transport within the active layer. The low dark current confirms minimal leakage and a well-formed diode junction, contributing to a high signal-to-noise ratio. The sharp increase in photocurrent with reverse bias reflects enhanced carrier extraction facilitated by the hybrid metal–oxide interlayer, which improves energy level alignment and reduces recombination losses, thereby enhancing overall photodetection efficiency and device stability [25].

Figure (3) shows the capacitance-voltage (C-V) characteristic in the dark, which is typical of a metal-insulator-semiconductor (MIS) or p-n junction device, revealing crucial information about its electrical behavior and internal structure. Over the negative voltage range (from -2.0 V to approximately 0 V), the capacitance remains relatively constant at a low value of about 70 nF/cm^2. This region, particularly if it were a high-frequency C-V plot of an MIS capacitor, would represent the accumulation or deep depletion regimes, where the applied bias maximizes the depletion region width or pushes the majority carriers toward the interface. As the voltage sweeps into the positive range, the capacitance begins a gradual increase, accelerating sharply near +1.5 V and culminating in a rapid, non-linear increase for voltages above +1.8 V, where it approaches and exceeds 3000 nF/cm^2. This sharp rise strongly suggests the onset of forward bias for a p-n junction or the strong inversion/accumulation regime, where the depletion width collapses (for a p-n junction) or the minority carrier concentration increases dramatically (for an MIS device) [20,21]. The inverse relationship between capacitance and depletion width, $C \propto 1/W_{dep}$, means the large capacitance corresponds to a minimal depletion width, which is expected at high forward bias. Analyzing the C^{-2} versus V plot (Mott-Schottky analysis), derived from this data, would allow for the calculation of the built-in potential and the doping concentration of the semiconductor layer, which are critical parameters for device modeling.

As shown in the C–V characteristics, capacitance is decreasing as the applied voltage shifts toward reverse bias. This trend indicates the gradual widening of the depletion region, which reduces charge storage capability and confirms the presence of a well-defined junction. The smooth, monotonic decrease in capacitance suggests uniform interfacial properties and minimal trap states at the hybrid metal–oxide and active layer interface. At forward bias, the capacitance increases due to charge accumulation, reflecting efficient carrier injection [26,27]. Overall, the C–V behavior confirms good interface quality, effective doping control, and stable electrical characteristics of the device.

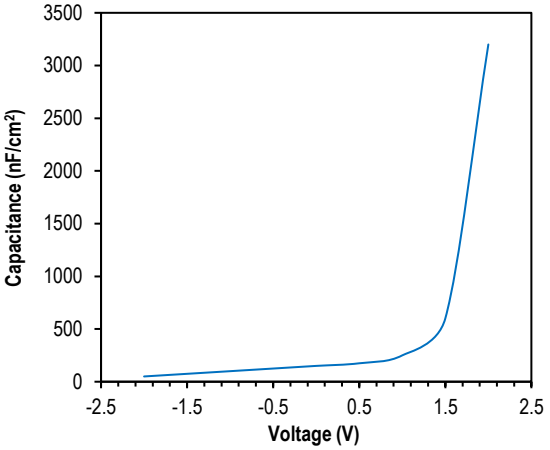

Fig. (3) The C-V characteristics in dark and under illumination for the device fabricated in this work

4. Conclusions

The electrical characterization, combining J-V and C-V analyses, leads to three key conclusions regarding the fabricated device, likely an organic photodiode. First, the J-V data confirms high-performance photodetection; a negligible dark current ensures a high signal-to-noise ratio, while a large saturation photocurrent under reverse bias demonstrates efficient light harvesting and charge extraction. Second, the C-V characteristics validate the formation of a high-quality junction; the strong voltage dependence of capacitance, particularly the decrease under reverse bias, confirms the gradual widening and collapse of a well-defined depletion region. Third, the low dark current and smooth C-V transition collectively indicate minimal leakage paths, good interface quality, and effective doping/charge control, which are crucial for the device's enhanced photodetection efficiency and stability, likely due to the optimized hybrid metal–oxide interlayer.

References

[1] J. Zhang et al., "Intermediate Phase Enhances Inorganic Perovskite and Metal Oxide Interface for Efficient Photovoltaics", *Joule*, 4(1) (2020) 222-234.

[2] M. Gao et al., "Photoluminescence manipulation in two-dimensional transition metal dichalcogenides", *J. Materiomics*, 9(4) (2023) 768-786.

[3] X. Zhang et al., "Recent advances in two-dimensional graphitic carbon nitride based photodetectors", *Mater. Design*, 235 (2023) 112405.

[4] Y. Han et al., "Solution processable transition metal dichalcogenides-based hybrids for photodetection", *Nano Mater. Sci.*, 1(4) (2019) 288-298.

[5] Q. Fu et al., "Versatile self-assembled monolayers for perovskite-based optoelectronic devices", *Mater. Today*, 89 (2025) 192-205.
[6] N. Pais, M.J. Shirodkar and P. Bhagavath, "Metal oxide doped organic thin film transistors: a comprehensive review", *Mater. Adv.*, 6(19) (2025) 6664-6681.
[7] X. Jia et al., "Pyro-phototronic effect enhanced self-powered photodetectors: A review on perovskite materials", *Next Mater.*, 8 (2025) 100563.
[8] A.S. AlShammari et al., "Effect of precursor concentration on the performance of UV photodetector using TiO_2/reduced graphene oxide (rGO) nanocomposite", *Results Phys.*, 19 (2020) 103630.
[9] M. Li et al., "High-temperature solid lubrication applications of Transition Metal Dichalcogenides (TMDCs) MX_2: A review", *Nano Mater. Sci.*, 7(4) (2025) 409-423.
[10] D. Tepatzi-Xahuentitla et al., "Structural and optical analysis of GaN and $In_xGa_{1-x}N$ photodetectors fabricated by PEALD on silicon", *Results Eng.*, 27 (2025) 106486.
[11] B. Robertson et al., "A comprehensive review on $MoSe_2$ nanostructures with an overview of machine learning techniques for supercapacitor applications", *RSC Adv.*, 14(51) (2024) 37644-37675.
[12] O.A. Hamadi, "Characteristics of CdO-Si Heterostructure Produced by Plasma-Induced Bonding Technique", *Proc. IMechE, Part L, J. Mater.: Design Appl.*, 222 (2008) 65-71.
[13] F. Rasch et al., "Highly selective and ultra-low power consumption metal oxide based hydrogen gas sensor employing graphene oxide as molecular sieve", *Sens. Actuat. B: Chem.*, 320 (2020) 128363.
[14] C. An et al., "Metal oxide-based supercapacitors: progress and prospectives", *Nanoscale Adv.*, 1(12) (2019) 4644-4658.
[15] S. Wu et al., "The evolution and future of metal halide perovskite-based optoelectronic devices", *Matter*, 4(12) (2021) 3814-3834.
[16] O.A. Hamadi, "Effect of Annealing on the Electrical Characteristics of CdO-Si Heterostructure Produced by Plasma-Induced Bonding Technique", *Iraqi J. Appl. Phys.*, 4(3) (2008) 34-37.
[17] A. Bukhtiar and B. Zou, "Low-dimensional II–VI semiconductor nanostructures of ternary alloys and transition metal ion doping: synthesis, optical properties and applications", *Mater. Adv.*, 5(17) (2024) 6739-6795.
[18] W. Xie et al., "Piezo-phototronic and pyro-phototronic effects enabled advanced high-performance metal halide perovskite optoelectronics", *Mater. Today Electron.*, 9 (2024) 100110.
[19] R. Kaur et al., "Metal-polypyridyl complexes mimicking electronic functions", *Coordin. Chem. Rev.*, 514 (2024) 215872.
[20] D. Liu et al., "Metal halide perovskite nanocrystals: application in high-performance photodetectors", *Mater. Adv.*, 2(3) (2021) 856-879.
[21] R.H. Turki and M.A. Hameed, "Spectral and Electrical Characteristics of Nanostructured NiO/TiO_2 Heterojunction Fabricated by DC Reactive Magnetron Sputtering", *Iraqi J. Appl. Phys.*, 16(3) (2020) 39-42.
[22] A. Liu et al., "Roadmap on metal-halide perovskite semiconductors and devices", *Mater. Today Electron.*, 11 (2025) 100138.
[23] J.H. Shin et al., "Large-scale growth of MoS_2 hybrid layer by chemical vapor deposition with nanosheet promoter", *Microelectron. Eng.*, 293 (2024) 112239.
[24] M.P. Shilpa et al., "Nonlinear optical and power limiting characteristics of noble metal decorated reduced graphene oxide and Ti_3C_2 MXene", *Carbon*, 235 (2025) 120025.
[25] M.A. Hameed, S.H. Faisal, R.H. Turki, "Characterization of Multilayer Highly-Pure Metal Oxide Structures Prepared by DC Reactive Magnetron Sputtering Technique", *Iraqi J. Appl. Phys.*, 16(4) (2020) 25-30
[26] Z. Wang et al., "Flexible near-infrared organic photodetectors for emergent wearable applications", *Wearable Electron.*, 1 (2024) 53-77.
[27] M. Banari et al., "CeO_2:ZnO hybrid nanorods for self-powered UV-photodetectors", *Ceram. Int.*, 51(1) (2025) 9-16.
[28] A.M. Hameed and M.A. Hameed, "Highly-Pure Nanostructured Metal Oxide Multilayer Structure Prepared by DC Reactive Magnetron Sputtering Technique", *Iraqi J. Appl. Phys.*, 18(4) (2022) 9-14.

